Lipopeptaibol Metabolites of *Tolypocladium geodes*: Total Synthesis, Preferred Conformation, and Membrane Activity

Mario Rainaldi,[a] Alessandro Moretto,[a] Cristina Peggion,[a] Fernando Formaggio,[a] Stefano Mammi,[a] Evaristo Peggion,[a] José Antonio Galvez,[b] Maria Dolores Díaz-de-Villegas,[b] Carlos Cativiela,[b] and Claudio Toniolo*[a]

Abstract: We have synthesized by solution methods and characterized the lipopeptaibol metabolite LP237-F8 extracted from the fungus *Tolypocladium geodes* and five selected analogues with the Etn → Aib or Etn → Nva replacement at position 8 and/or a triple Gln → Glu(OMe) replacement at positions 5, 6, and 9 (Etn = *Cα*-ethylnorvaline, Aib = *α*-aminoisobutyric acid, Nva = norvaline). Conformation analysis, performed by FT-IR absorption, NMR, and CD techniques, strongly supports the view that the six terminally blocked decapeptides are highly helical in solution. Helix topology and amphiphilic character are responsible for their remarkable membrane activity. At position 8 the combination of high hydrophobicity and C*α* tetrasubstitution, as in the Etn-containing LP237-F8 metabolite, has a positive effect on membrane interaction.

Keywords: antitumor agents · conformation analysis · peptaibols · peptides · total synthesis

Introduction

Peptaibols are a unique class of membrane-active metabolites of fungal origin.[1, 2] These antibiotic peptides are characterized by a linear sequence of *α*-amino acids, a high population of the C*α*,*α*-disubstituted glycine *α*-aminoisobutyric acid (Aib), an N-terminal acetyl group, and a C-terminal 1,2-amino alcohol. In the last few years a variety of peptides have been sequenced that bear a fatty acyl moiety linked to the N-terminal amino acid as a new characteristic feature for peptaibols.[3, 4] These peptides are referred to *lipopeptaibols* because of the lipophilic character of the N-terminal group. They were isolated from cultures of the fungi *Trichoderma longibrachiatum* (trichogin), *Trichoderma koningii* (trikoningins), *Trichoderma viride* (trichodecenins), *Trichoderma polysporum* (trichopolyns), *Mycogone rosea* (helioferins), and *Tolypocladium geodes* (metabolites LP237). Typically, most of them exhibit microheterogeneity, that is, the natural mixtures contain a series of closely related peptides with a limited number of conservative variations in the sequence.

In particular, in the course of a recent screening program for fungal metabolites exhibiting antitumor activity, the highly cytotoxic peptides LP237-F5, -F7, and -F8 were isolated and sequenced[5, 6] (Scheme 1). The *n*-octanoyl (Oc) N*α*-blocked and leucinol (Lol) C*α*-blocked 10-mer peptide F8 was found to be the main component of the bioactive mixture. In addition to the frequently observed achiral Aib, another member of the family of C*α*,*α*-disubstituted glycines, the chiral *Cα*-ethylnorvaline (Etn) residue, was shown to occur in

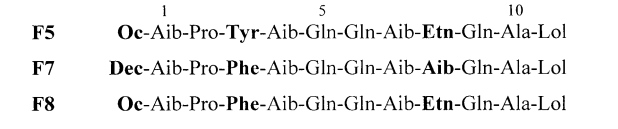

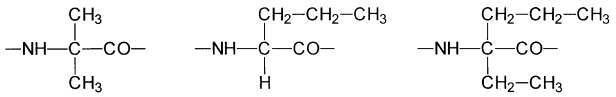

Scheme 1. Amino acid sequences of the lipopeptaibol metabolites LP237-F5, -F7, and -F8. All the *α*-amino acids and the 1,2-amino alcohol have the *S* configuration. At the N-terminal acyl moiety and at positions 3 and 8, variations in the sequence are indicated in bold. The chemical formulae of Nva and the two C*α*-tetrasubstituted *α*-amino acids are also shown. Aib = *α*-aminoisobutyric acid, Dec = *n*-decanoyl, Etn = C*α*-ethylnorvaline, Lol = leucinol, Nva = norvaline, Oc = *n*-octanoyl.

[a] Prof. C. Toniolo, M. Rainaldi, Dr. A. Moretto, Dr. C. Peggion, Prof. F. Formaggio, Prof. S. Mammi, Prof. E. Peggion
Institute of Biomolecular Chemistry, CNR
Department of Organic Chemistry, University of Padova
via Marzolo 1, 35131 Padova (Italy)
Fax: (+39) 49-827-5239
E-mail: claudio.toniolo@unipd.it

[b] Dr. J. A. Galvez, Dr. M. D. Díaz-de-Villegas, Prof. C. Cativiela
Departamento de Quimica Organica y Quimica Fisica
Instituto de Ciencia de Materiales de Aragon
Universidad de Zaragoza, CSIC
50009 Zaragoza (Spain)

 DOI: 10.1002/chem.200304756 © 2003 Wiley-VCH Verlag GmbH & Co. KGaA, Weinheim

the F5 and F8 primary structures. To our knowledge, this latter α-amino acid has not previously been reported as a component of a terrestrial product. However, it has been found in extraterrestrial sediments such as the Murchison meteorite.[7] Unfortunately, in none of these works has the absolute configuration of the Etn residue been assessed. Etn has been synthesized (in the racemic form) and shown to behave as a competitive inhibitor of methionine.[8] The F5, F7, and F8 metabolites differ by the N-terminal acyl moiety (Oc or decanoyl (Dec)) and the α-amino acids in positions 3 (Tyr or Phe) and 8 (Etn or Aib).

Herein we describe the total synthesis, conformation analysis (by FT-IR absorption, NMR, and CD techniques) in solution, and membrane permeability measurements of the lipopeptaibol metabolite LP237-F8 (**c′** in Scheme 2). We decided to incorporate Etn as the *S* enantiomer because of its greater availability; the asymmetric synthesis of this enantiomer is also reported here. In addition, we have examined the effects induced by hydrophobicity (higher in Etn and norvaline (Nva) than in Aib) and Cα substitution[9] (higher in Aib and Etn than in Nva) at position 8 (analogues **a′** and **b′** in Scheme 2). Finally, the spectroscopic and biophysical properties of peptides **a′**–**c′** have been compared with those of their synthetic precursors (peptides **a**–**c** in Scheme 2), which are characterized by three Glu(OMe) residues with an ester side-chain functionality in place of the three Gln residues with a primary amide side-chain functionality at positions 5, 6, and 9.

(**a**) Oc-Aib-Pro-Phe-Aib-[**Glu(OMe)**]$_2$-Aib-**Aib**-**Glu(OMe)**-Ala-Lol

(**b**) Oc-Aib-Pro-Phe-Aib-[**Glu(OMe)**]$_2$-Aib-**Nva**-**Glu(OMe)**-Ala-Lol

(**c**) Oc-Aib-Pro-Phe-Aib-[**Glu(OMe)**]$_2$-Aib-**Etn**-**Glu(OMe)**-Ala-Lol

(**a'**) Oc-Aib-Pro-Phe-Aib-(**Gln**)$_2$-Aib-**Aib**-**Gln**-Ala-Lol

(**b'**) Oc-Aib-Pro-Phe-Aib-(**Gln**)$_2$-Aib-**Nva**-**Gln**-Ala-Lol

(**c'**) Oc-Aib-Pro-Phe-Aib-(**Gln**)$_2$-Aib-**Etn**-**Gln**-Ala-Lol

Scheme 2. Amino acid sequences of the peptides investigated in this work. Peptide **c′** corresponds to the lipopeptaibol LP237-F8. All α-amino acids and the 1,2-amino alcohol have the *S* configuration.

Abstract in Italian: *Abbiamo sintetizzato in soluzione e caratterizzato il metabolita lipopeptaibolico LP237-F8 estratto dal fungo Tolypocladium geodes e cinque suoi analoghi recanti la sostituzione Etn → Aib o Etn → Nva in posizione 8 e la tripla sostituzione Gln → Glu(OMe) nelle posizioni 5, 6 e 9. La nostra indagine conformazionale, condotta con le tecniche dell'assorbimento IR, NMR e CD, indica chiaramente che i sei decapeptidi bloccati alle funzioni N- e C- terminali assumono un'alta percentuale di forma elicoidale in soluzione. La natura elicoidale e il carattere anfifilico sembrano essere i fattori responsabili della loro elevata attività sulle membrane. In posizione 8 la combinazione di una elevata idrofobicità e della tetrasostituzione all'atomo Cα ha un effetto positivo sull'interazione con le membrane.*

Abstract in Spanish: *Utilizando metodos sintéticos en disolución se ha preparado y caracterizado el metabolito lipopeptaibol LP237-F8 extraído del hongo Tolypocladium geodes, así como cinco análogos en los que el residuo Etn en posición 8 ha sido sustituido por Aib o Nva y una triple Gln → Glu(OMe) sustitución ha sido introducida en las posiciones 5, 6 y 9. El análisis conformacional realizado mediante FT-IR, NMR y CD pone claramente de manifesto que los seis decapéptidos muestran una alta helicidad en solución. La topología helicoidal y el carácter amfifílico son responsables de su importante actividad de membrana. Como ocurre en el metabolito F8 que contiene Etn, la combinación de la alta hidrofobicidad y la tetrasustitución en Cα del residuo en posición 8 tiene un efecto positivo en la interacción con la membrana.*

Results and Discussion

Synthesis and characterization: Preparation of (*S*)-Etn was performed by extension of our general chemical methodology developed for the synthesis of Cα-tetrasubstituted α-amino acids.[10] Diastereoselective alkylation of chiral (1′*S*,2′*R*,4′*R*)-10′-(dicyclohexylsulfamoyl)isobornyl 2-cyanobutanoate (**1**) with allyl bromide according to our previously described methodology[11] cleanly affords the corresponding allylated compound (**2**; Scheme 3) in 92% yield as a 90:10 mixture in which the diastereoisomer with *S* configuration at the C2 position predominates; this diastereoisomer is derived from the formation of a chelated *Z* enolate and attack by the electrophile from the Cα-*Re* side, opposite to the 10′-(dicyclohexylsulfamoyl) group. The diastereomeric ratio of the product was determined in the crude reaction mixture by integration of the ^{13}C NMR absorptions (75 MHz) of the vinylic carbon atoms at about $\delta = 130.7$ ppm. The major diastereoisomer can be easily isolated from the mixture by crystallization from MeOH and further elaborated to afford (*S*)-Etn (**5**) according to Scheme 3. Hydrogenation of the alkene moiety of **2** under 1 atm of hydrogen with palladium on charcoal yielded the corresponding saturated compound **3**. Basic hydrolysis of the ester group with potassium hydroxide in MeOH followed by synthesis of the α-cyanoacylazide and subsequent Curtius rearrangement gave the corresponding urethane **4**. Finally, acidic hydrolysis afforded (*S*)-Etn (**5**) as the hydrochloride salt in enantiomerically pure form and with a 68% yield from the *S* cyanoester. Ion-exchange chromatography released the free amino acid.

Since we expected potentially difficult peptide-coupling steps, particularly those required for the incorporation of the Cα-tetrasubstituted α-amino acids Etn and Aib,[12] the total chemical syntheses of the metabolite LP237-F8 (peptide **c′**) and its Aib (peptide **a′**) and Nva (peptide **b′**) analogues were carried out either by the EDC/HOBt method[13] or the EDC/HOAt method[14] (Scheme 4). Originally, we decided to take advantage of the racemization-free, step-by-step synthetic strategy. However, we were forced to limit such a strategy to the protected hexapeptide level because of the relatively small amount of (*S*)-Etn available. In any case, by using this approach we were able to exploit a series of short sequences which proved to be useful to investigate the role of main-chain lengthening on peptide conformation (see below). The methyl ester group of the Z-Ala-Leu-OMe dipeptide was reduced to

© 2003 Wiley-VCH Verlag GmbH & Co. KGaA, Weinheim

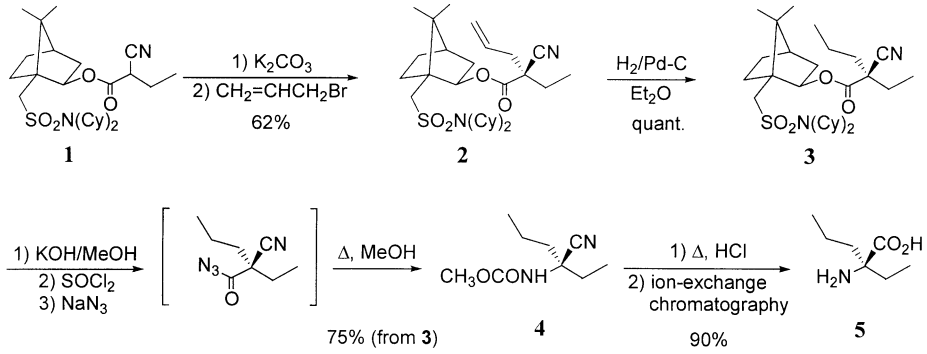

Scheme 3. Asymmetric synthesis of (*S*)-Etn (**5**). Cy = cyclohexyl.

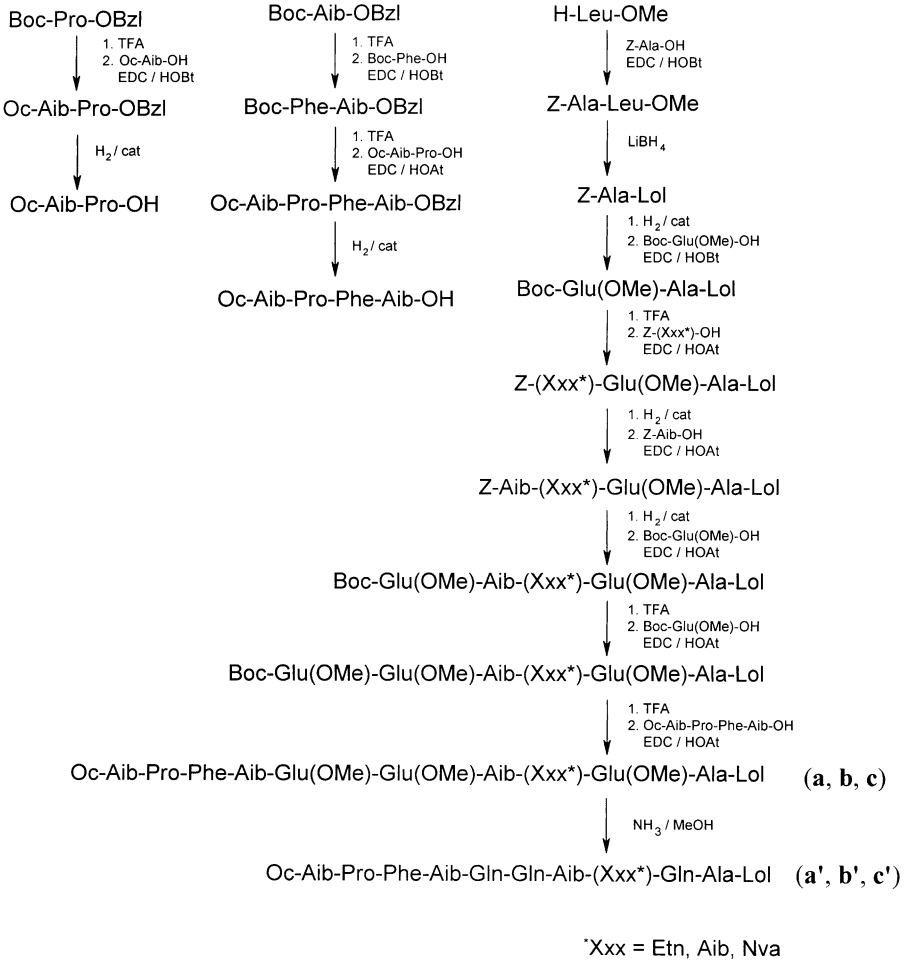

Scheme 4. Strategy for the synthesis of the lipopeptaibol LP237-F8 (**c′**) and its five analogues (**a**–**c**, **a′**, and **b′**). Boc = *tert*-butyloxycarbonyl, Bzl = benzyl, EDC = *N*-ethyl-*N*′-[3-(dimethylamino)propyl]carbodiimide, HOAt = 7-aza-1-hydroxy-1,2,3-benzotriazole, HOBt = 1-hydroxy-1,2,3-benzotriazole, TFA = trifluoroacetic acid, Z = benzyloxycarbonyl.

primary alcohol (Z-Ala-Lol) by using $LiBH_4$, which does not interfere with the peptide and urethane functions.[15] Removal of the Boc and Z Nα-protecting groups was achieved by mild acidolysis (diluted TFA) and catalytic hydrogenolysis, respectively. During the course of the synthesis, the difficult-to-handle Gln residues were replaced by Glu(OMe) residues. This approach also allowed us to synthesize three Glu(OMe)-based analogues of peptides **a′**–**c′**, namely peptides **a**–**c**. However, this strategy forced us to reduce the C-terminal ester function at the dipeptide stage immediately before incorporation of the first Glu(OMe) residue. To avoid the possible competition between the N-terminal amino group of the growing peptide chain and the C-terminal Lol alcohol function during the various peptide bond formation steps, we took advantage of the higher nucleophilicity of the amino function. To this end we slowly added the solution containing a slight excess of the acylating reagent to the solution of the α-amino peptide alcohol. The strategy for the syntheses of the protected tetrapeptide fragment and the decapeptides **a**–**c** was chosen in such a way as to minimize racemization. In particular: 1) the C-terminal Pro residue of the dipeptide carboxylic acid, being N-alkylated, cannot form the 5(4*H*)-oxazolone intermediate and 2) the C-terminal Aib residue of the tetrapeptide carboxylic acid is achiral. Conversion of the Glu(OMe) decapeptides **a**–**c** into the corresponding Gln peptides **a′**–**c′** was obtained by triple ester aminolysis in anhydrous MeOH.[16] The progress of this latter reaction was monitored by reverse-phase HPLC. The reaction was slow and took several days for completion. The overall yields for the synthesis of decapeptides **a′**, **b′**, and **c′** were 13, 18, and 10%, respectively.

The purities of the newly synthesized intermediates and final synthetic products were assessed by TLC in three different solvent systems, solid-state IR absorption spectroscopy, ESI-TOF mass spectrometry (the latter technique was only used for peptides **a**–**c** and **a′**–**c′**), and ^{1}H NMR spectroscopy (Table 1).

Conformation analysis in solution: A detailed investigation of the preferred conformation in solution of the lipopeptaibol metabolite LP237-F8 (peptide **c′**) and its analogues (**a′**, **b′**, and

 © 2003 Wiley-VCH Verlag GmbH & Co. KGaA, Weinheim

Table 1. Physical properties and analytical data for the newly synthesized peptides.

Compound[a]	Yield [%]	M.p. [°C][b]	Purification[c]	TLC[d] R_f(I)	R_f(II)	R_f(III)	$[M+H]^+_{calcd}$/ $[M+H]^+_{exp}$[e]	IR $\tilde{\nu}$ [cm^{-1}][f]
Z-Etn-OH	79	oil	EtOAc/PE	0.40	0.90	0.25	–	3472, 3410, 1704, 1678, 1522
Z-Ala-Lol	89	90–91	EtOAc/PE	0.65	0.90	0.40	–	3317, 1711, 1690, 1653, 1531
Boc-Glu(OMe)-Ala-Lol	87	waxy solid	f.c.	0.60	0.90	0.30	–	3308, 1745, 1711, 1682, 1666, 1522
Z-Aib-Glu(OMe)-Ala-Lol	79	waxy solid	f.c.	0.60	0.85	0.25	–	3305, 1751, 1721, 1654, 1540
Z-Etn-Glu(OMe)-Ala-Lol	69	waxy solid	f.c.	0.55	0.85	0.20	–	3309, 1745, 1724, 1658, 1533
Z-Nva-Glu(OMe)-Ala-Lol	88	waxy solid	f.c.	0.65	0.90	0.35	–	3313, 1738, 1666, 1537
Z-Aib-Aib-Glu(OMe)-Ala-Lol	76	waxy solid	f.c.	0.60	0.90	0.15	–	3290, 1747, 1704, 1678, 1637, 1543
Z-Aib-Etn-Glu(OMe)-Ala-Lol	76	waxy solid	f.c.	0.60	0.90	0.15	–	3310, 1734, 1714, 1653, 1644, 1541
Z-Aib-Nva-Glu(OMe)-Ala-Lol	81	waxy solid	f.c.	0.65	0.90	0.25	–	3307, 1751, 1708, 1662, 1639, 1514
Boc-Glu(OMe)-Aib-Aib-Glu(OMe)-Ala-Lol	74	waxy solid	f.c.	0.65	0.85	0.10	–	3311, 1731, 1664, 1657, 1538
Boc-Glu(OMe)-Aib-Etn-Glu(OMe)-Ala-Lol	69	waxy solid	f.c.	0.60	0.85	0.10	–	3317, 1740, 1664, 1660, 1532
Boc-Glu(OMe)-Aib-Nva-Glu(OMe)-Ala-Lol	72	waxy solid	f.c.	0.70	0.90	0.15	–	3315, 1739, 1660, 1542
Boc-[Glu(OMe)]$_2$-Aib-Aib-Glu(OMe)-Ala-Lol	68	waxy solid	f.c.	0.65	0.85	0.15	–	3314, 1745, 1659, 1541
Boc-[Glu(OMe)]$_2$-Aib-Etn-Glu(OMe)-Ala-Lol	69	waxy solid	f.c.	0.60	0.85	0.10	–	3308, 1751, 1712, 1664, 1521
Boc-[Glu(OMe)]$_2$-Aib-Nva-Glu(OMe)-Ala-Lol	76	waxy solid	f.c.	0.65	0.90	0.20	–	3312, 1745, 1708, 1657, 1531
Oc-Aib-Pro-OBzl	78	oil	f.c.	0.90	0.95	0.45	–	3308, 1736, 1664, 1525
Boc-Phe-Aib-OBzl	87	91–92	EtOAc/PE	0.90	0.95	0.55	–	3311, 1744, 1655, 1537
Oc-Aib-Pro-Phe-Aib-OBzl	75	oil	f.c.	0.70	0.90	0.35	–	3308, 1746, 1712, 1661, 1649, 1524
Oc-Aib-Pro-Phe-Aib-[Glu(OMe)]$_2$-Aib-Aib-Glu(OMe)-Ala-Lol	66	waxy solid	f.c.	0.70	0.90	0.30	1328.8463/ 1328.8494	3309, 1743, 1655, 1529
Oc-Aib-Pro-Phe-Aib-[Glu(OMe)]$_2$-Aib-Etn-Glu(OMe)-Ala-Lol	58	waxy solid	f.c.	0.70	0.90	0.20	1370.8955/ 1370.8986	3313, 1740, 1662, 1537
Oc-Aib-Pro-Phe-Aib-[Glu(OMe)]$_2$-Aib-Nva-Glu(OMe)-Ala-Lol	65	waxy solid	f.c.	0.65	0.85	0.25	1342.8718/ 1342.8749	3307, 1741, 1649, 1519
Oc-Aib-Pro-Phe-Aib-(Gln)$_2$-Aib-Aib-Gln-Ala-Lol	98	waxy solid	f.c.	0.45	0.80	0.10	642.9157/ 642.9172[g]	3311, 1669, 1661, 1537
Oc-Aib-Pro-Phe-Aib-(Gln)$_2$-Aib-Etn-Gln-Ala-Lol	97	waxy solid	f.c.	0.50	0.85	0.15	1325.9617/ 1325.9648	3315, 1661, 1657, 1527
Oc-Aib-Pro-Phe-Aib-(Gln)$_2$-Aib-Nva-Gln-Ala-Lol	98	waxy solid	f.c.	0.40	0.85	0.10	1297.8457/ 1297.8488	3322, 1656, 1647, 1525

[a] All α-amino acids and the 1,2-amino alcohol have the *S* configuration. [b] Determined on a Leitz model Laborlux 12 apparatus (Wetzlar, Germany). [c] Purification was either by recrystallization from the given solvent(s) (EtOAc = ethyl acetate, PE = petroleum ether) or by flash chromatography (f.c.; silica gel 60, 40–63 mesh, Merck, Darmstadt, Germany). [d] TLC on silica gel 60F plates (Merck) in the following solvent systems: I) chloroform/ethanol (9:1), II) butan-1-ol/water/acetic acid (3:1:1), III) toluene/ethanol (7:1); the plates were developed with a UV lamp or with the hypochlorite/starch/iodide chromatic reaction, as appropriate; a single spot was observed in each case. [e] Determined on a Perseptive Biosystems model Mariner ESI-TOF mass spectrometer (Foster City, CA). [f] Determined in KBr pellets on a Perkin-Elmer 580B spectrophotometer (Norwalk, CT) equipped with a Perkin Elmer 3600 IR data station. [g] $[(M+2H)/2]_{calcd}/[(M+2H)/2]_{exp}$.

a–**c**) was carried out by using FT-IR absorption, two-dimensional NMR, and CD techniques in solvents of different polarity.

The conformational preferences of the C-terminal, Nα-protected peptides (up to the hexamer) were investigated in a structure-supporting solvent ($CDCl_3$) by FT-IR absorption spectroscopy over the peptide concentration range 10–0.1 mM. Representative spectra (for short sequences of peptide **a**) in the most informative N–H stretching (amide A) region (peptide concentration: 1 mM) are illustrated in Figure 1. The curves are characterized by two bands, at about 3425 cm^{-1} (free, solvated NH groups) and 3355–3310 cm^{-1} (strongly hydrogen-bonded NH groups of folded conformations).[17–19] The intensity of the low-frequency band relative to that of the high-frequency band increases significantly as main-chain length increases. We have also been able to demonstrate that, even at a concentration of 10 mM, self-association through intermolecular N–H···O=C hydrogen bonding is negligible (less than 5%) for all oligomers. (Figure 1 shows the close similarity between the spectra of the longest peptide in this series at the two concentrations.) Therefore, the observed hydrogen bonding should be interpreted as arising almost exclusively from intramolecular N–H···O=C interactions. As the low-frequency band is clearly seen in the Nα-protected dipeptide amino alcohol

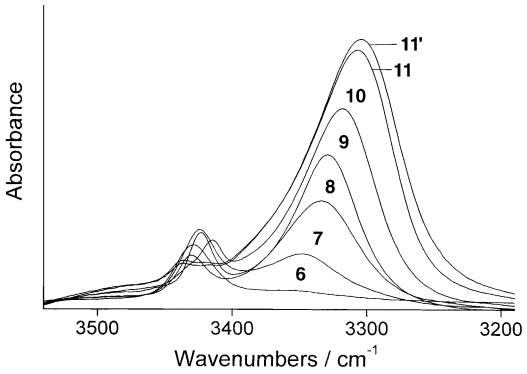

Figure 1. FT-IR absorption spectra in the 3500–3200 cm^{-1} region for the C-terminal short sequences Z-Ala-Lol (**6**), Boc-Glu(OMe)-Ala-Lol (**7**), Z-Aib-Glu(OMe)-Ala-Lol (**8**), Z-(Aib)$_2$-Glu(OMe)-Ala-Lol (**9**), Boc-Glu(OMe)-(Aib)$_2$-Glu(OMe)-Ala-Lol (**10**), and Boc-[Glu(OMe)]$_2$-(Aib)$_2$-Glu(OMe)-Ala-Lol (**11**) of peptide **a** in $CDCl_3$ solution. Peptide concentration: 1 mM. Spectrum **11′** is the spectrum of the hexapeptide at 10 mM peptide concentration.

© 2003 Wiley-VCH Verlag GmbH & Co. KGaA, Weinheim

(**7**) but not in the shorter Z-Ala-Lol (**6**), it is reasonable to exclude the possibility that the preferred folded conformation would be of the γ-bend type.[20]

The FT-IR absorption analysis provided evidence that intramolecular hydrogen bonding typical of α[21, 22] or β[23–25]-turn conformations is the predominant feature of the C-terminal sequences of these lipopeptaibols in $CDCl_3$ solution.

The FT-IR absorption spectra of the lipopeptaibols **a**–**c** and **a′**–**c′** in $CDCl_3$ solutions (peptide concentrations: 1 and 0.1 mM) are shown in Figure 2. They are dominated by a very strong band at about 3325 cm^{-1}. Additional bands (shoulders) are barely visible at wavenumbers $>3400\ cm^{-1}$. A modest decrease in the relative intensity of the 3325 cm^{-1} band is observed between the spectra recorded at 1 and 0.1 mM concentrations; this is indicative of the contribution of a minor amount of intermolecular hydrogen bonds. In any case, at the lower concentration examined (0.1 mM) the 3325 cm^{-1} band is still very intense in all of these decapeptides, which supports the view that they are characterized by an extensive set of intramolecular C=O ··· H–N hydrogen bonds. From our FT-IR absorption analysis it may be concluded that in $CDCl_3$ solution all the lipopeptaibols examined tend to fold in an intramolecularly hydrogen-bonded structure. However, this technique alone did not allow us to unambiguously determine the nature of the helix that is formed.

The NMR spectroscopic investigation of the conformation of lipopeptaibol **a′** was carried out in an aqueous sodium dodecylsulfate (SDS) solution. The combined analysis of TOCSY and NOESY spectra led to the complete assignment of all proton resonances. In spite of the presence of a Pro residue at position 2, no evidence of *cis*/*trans* isomerism about the Aib^1–Pro^2 bond was found in the NMR spectra. The complete proton assignment is reported in Table 2. The assignment of the methyl groups of the Aib residues is based

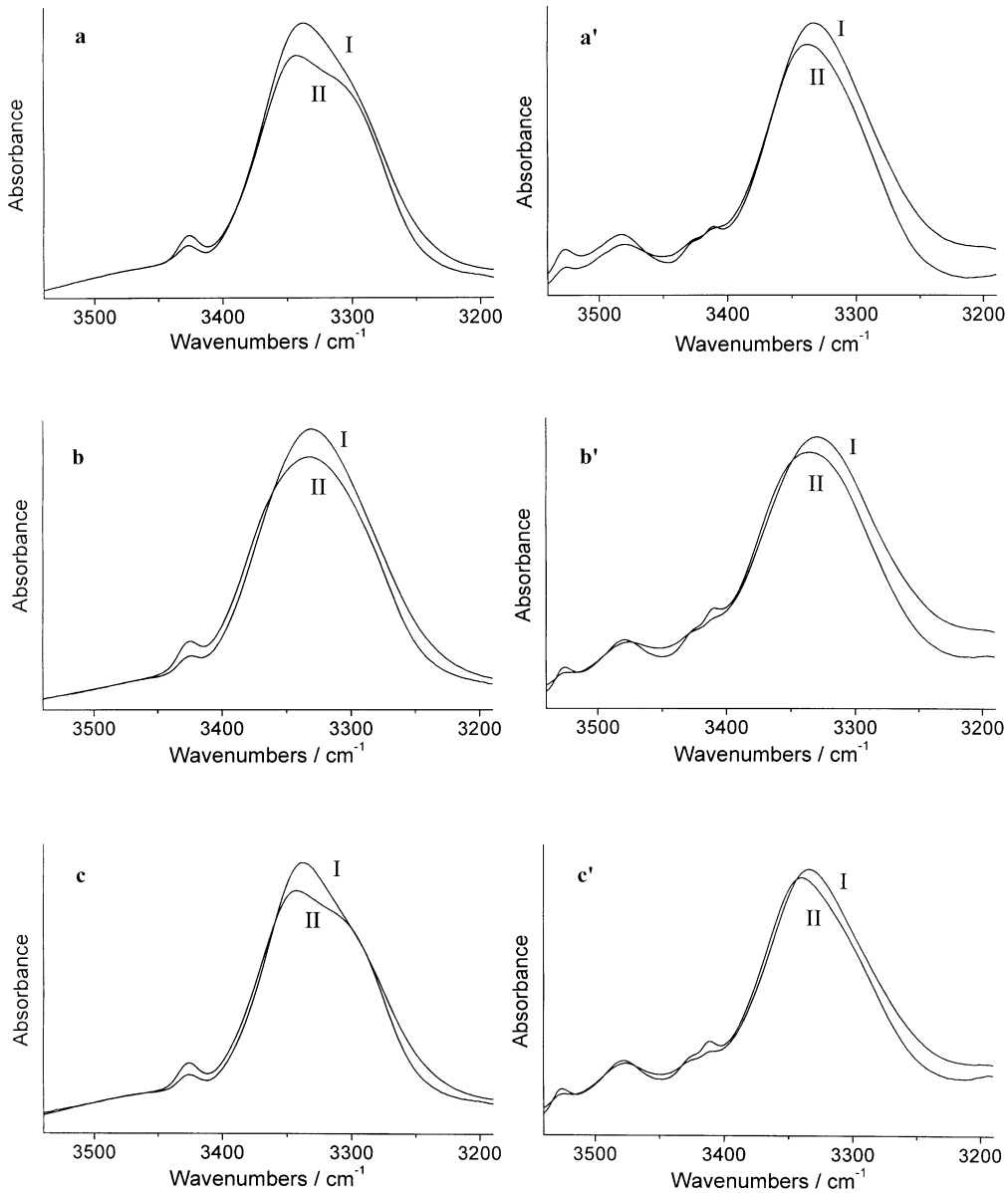

Figure 2. FT-IR absorption spectra in the 3500–3200 cm^{-1} region for peptides **a**–**c** and **a′**–**c′** in $CDCl_3$ solution at peptide concentrations of 1 mM (I) and 0.1 mM (II).

 © 2003 Wiley-VCH Verlag GmbH & Co. KGaA, Weinheim

Table 2. Proton chemical shift values (ppm) at 313 K relative to tetramethylsilane and temperature dependencies of amide proton chemical shift values (ppb K^{-1}) for peptide **a′**.

Residue	$^{\alpha}$H	$^{\beta}$H	$^{\gamma}$H	$^{\delta}$H	$^{\varepsilon}$H	H aromatic	HN	$\Delta\delta/\Delta T$
Aib[1]		1.60, 1.61					8.48	5.6 ± 0.2
Pro[2]	4.47	2.32, 1.43	2.00, 1.88	4.04, 3.47				
Phe[3]	4.66	3.35, 3.19				7.28, 7.41	8.13	3.8 ± 0.1
Aib[4]		1.52, 1.69					7.96	1.9 ± 0.1
Gln[5]	4.11	2.19	2.58, 2.51		7.47, 6.83		8.02	6.7 ± 0.3
Gln[6]	4.16	2.18, 2.25	2.51		7.42, 6.78		7.88	4.1 ± 0.1
Aib[7]		1.66					8.01	4.5 ± 0.1
Aib[8]		1.57, 1.64					7.86	5.6 ± 0.1
Gln[9]	4.14	2.28	2.70, 2.60		7.37, 6.76		7.73	4.0 ± 0.1
Ala[10]	4.41	1.62					7.95	2.4 ± 0.1
Lol	4.16	1.49, 1.38	1.81	0.98			7.08	3.0 ± 0.1
		3.69, 3.60						

on the analysis of the NOESY spectrum alone, on the assumption that the helix formed (see below) would be right-handed. The summary of the interresidue NOESY connectivities is presented in Figure 3. The presence of strong NH(i)–NH($i+1$) peaks almost throughout the sequence, accompanied by weak αH(i)–NH($i+1$) peaks, is an indication that the

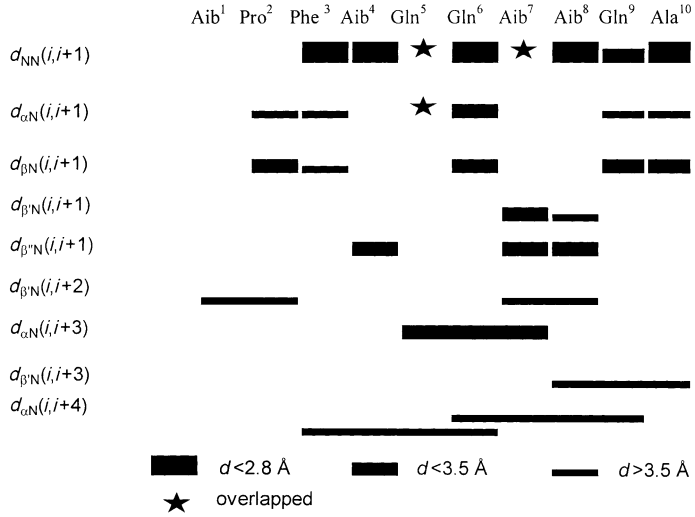

Figure 3. Interresidue NOEs found for peptide **a′**. The thickness of the bar reflects the integrated intensity of the peak, as the scale at the bottom shows.

peptide might adopt a helical conformation. Of the four possible αH(i)–NH($i+3$) peaks, only one was detected (Figure 4). In a right-handed helical conformation, the *pro-R* methyl protons β' of the Aib residues are in close proximity with the NH protons of residues one turn away.[26] Again, of the four possible β'H(i)–NH($i+3$) peaks, only one was detected (outside the section shown in Figure 4). These findings support the presence of a helical conformation only in part and indicate that such an arrangement is probably in equilibrium with other conformers. Two αH(i)–NH($i+4$) connectivities suggest that the α-helix conformation is indeed populated. Two β'H(i)–NH($i+2$) peaks were also found. The first one is around Pro[2] and could arise from a β-turn conformation. The other one, toward the C terminus, could be due to a transient 3_{10}-helical arrangement. The temperature

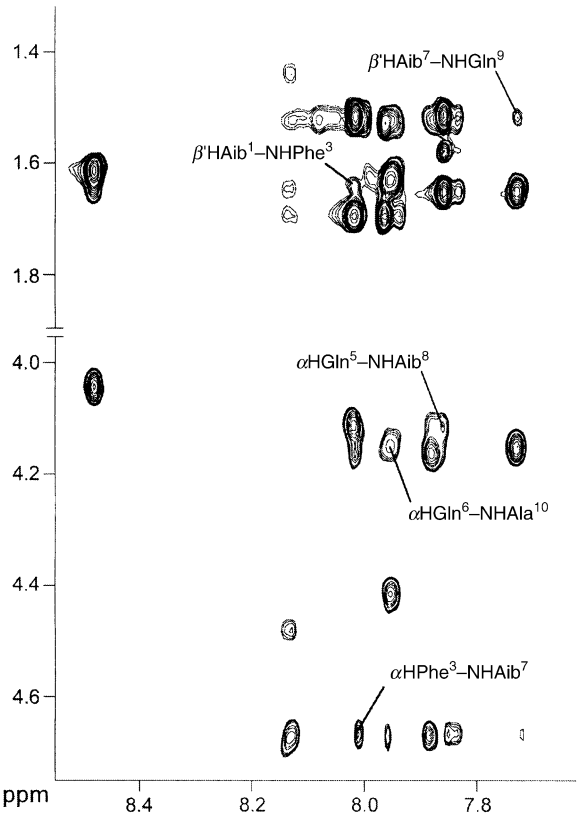

Figure 4. Section of the NOESY spectrum of peptide **a′**. The medium-range $d_{\alpha N}(i, i+4)$ and $d_{\alpha N}(i, i+2)$ cross-peaks are indicated.

dependence of the amide protons is also reported in Table 2. The protons of residues Phe[3], Aib[4], Gln[9], Ala[10], and Lol show a small temperature dependence ($\Delta\delta/\Delta T \leq 4.0$ ppb K^{-1}), which is usually interpreted as indicating the presence of intramolecular hydrogen bonds.

Extensive molecular dynamics calculations resulted in a family of 32 accepted structures with violations to the NOE restraints lower than 0.4 Å. A superimposition of these structures is shown in Figure 5. The average values of the

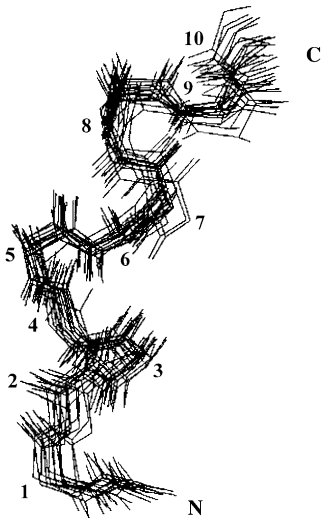

Figure 5. Overlay of the 32 minimized structures of peptide **a′**. Amino acid numbering is indicated. Sinde chains are omitted.

© 2003 Wiley-VCH Verlag GmbH & Co. KGaA, Weinheim

Table 3. Average values of φ,ψ backbone torsion angles, their relative standard deviations, and order parameters resulting from the 32 calculated structures of peptide **a′**.

Residue	Angle	Average value and standard deviation	Order parameter
Aib[1]	φ	-80.2 ± 5.4	0.996
Aib[1]	ψ	-53.2 ± 3.5	0.998
Pro[2]	φ	-84.1 ± 3.8	0.998
Pro[2]	ψ	13.5 ± 1.4	1
Phe[3]	φ	-91.7 ± 8.6	0.989
Phe[3]	ψ	-9.6 ± 1.4	1
Aib[4]	φ	-83.1 ± 2	0.999
Aib[4]	ψ	-48.3 ± 6	0.995
Gln[5]	φ	-86.3 ± 8.3	0.99
Gln[5]	ψ	-12.6 ± 2.1	0.978
Gln[6]	φ	-77.1 ± 6.7	0.993
Gln[6]	ψ	-26.4 ± 4	0.998
Aib[7]	φ	-75.7 ± 4.4	0.997
Aib[7]	ψ	-42 ± 6.4	0.994
Aib[8]	φ	-89 ± 30.9	0.88
Aib[8]	ψ	-38.5 ± 7.8	0.991
Gln[9]	φ	-77.2 ± 15.2	0.967
Gln[9]	ψ	-15.5 ± 11.5	0.981
Ala[10]	φ	-83.2 ± 19.2	0.946
Ala[10]	ψ	-8.5 ± 12.5	0.977
Lol	φ	108.4 ± 59.4	0.655

φ,ψ angles recovered from the dynamics are reported in Table 3 together with their standard deviations. These deviations are very small, as is also indicated by the values of the order parameter, which are very close to one. This is evidence for a strong tendency toward the average structure, which is a slightly distorted α helix from residue Aib[4] to Ala[10]. The distortion is mainly due to the unusual values of the φ angles, which vary from -76° to -89°. The difference from the canonical value of -63° is nevertheless not high. As expected, the C terminus experiences a higher degree of conformational averaging, as indicated by the lower order parameters already observed at the level of Aib[8]. At the N terminus, the distortion is greater, very likely because of the presence of the Pro residue at position 2. The angles of residues Aib[1] and Pro[2] are compatible with the presence of a type-I β turn.

Table 4 summarizes the intramolecular hydrogen bonds found in the 32 accepted structures. The amide protons significantly involved in such bonds are those of Phe[3], Gln[9], Ala[10], and Lol. The agreement with the results of the variable temperature study is quite reasonable. Indeed, the temperature coefficient of these NH protons is ≤ 4.0 ppb K^{-1}. Only the Aib[4] NH proton, which exhibits the lowest temperature dependence in the entire sequence, is not found to form intramolecular hydrogen bonds in the dynamics calculations. A possible explanation for this result could be that this particular proton is in part shielded from the solvent for different reasons, for example by the Phe ring or by the *n*-octanoyl N-terminal chain.

Table 4. Intramolecular C=O···H–N hydrogen bonds found in the 32 calculated structures of peptide **a′**.[a]

NH donor	O acceptor	Occurrence
Phe[3]	Oc	12
Aib[7]	Phe[3]	2
Aib[8]	Gln[5]	1
Gln[9]	Gln[5]	8
Ala[10]	Gln[6]	10
Ala[10]	Aib[7]	1
Lol	Aib[8]	6

[a] The maximum hydrogen–acceptor distance was set to 2.4 Å. The donor–hydrogen–acceptor angle was 145°.

The far-UV CD spectra of the six lipopeptaibols **a**–**c** and **a′**–**c′** in MeOH solution (Figure 6) are very similar, with a negative maximum at 208 nm (peptide $\pi \rightarrow \pi^*$ exciton split

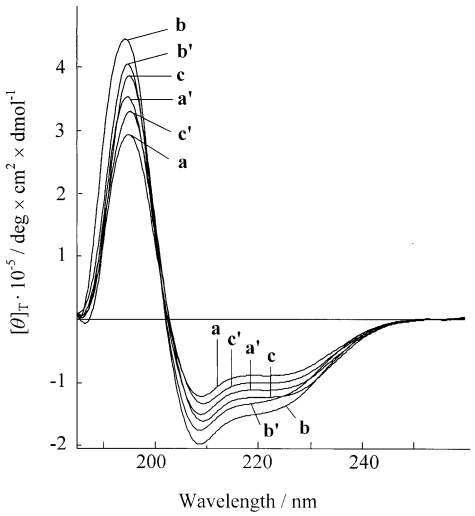

Figure 6. Far-UV CD spectra of the lipopeptaibol LP237-F8 (**c′**) and its five analogues (**a**–**c**, **a′**, and **b′**) in MeOH solution.

component) and a pronounced negative shoulder in the vicinity of 222 nm (peptide $n \rightarrow \pi^*$ transition).[27] The conformationally sensitive $[\theta]_T^{222}/[\theta]_T^{208}$ ratio R is approximately 0.7, a fact indicating that the right-handed helix adopted in this solvent is predominantly of the α type.[28–30] In 1,1,1,3,3,3-hexafluoroisopropanol solution (spectra not shown) the R value (≈ 0.95) suggests a further increase in the α-helix population. By applying the conventional criteria for the determination of the percentage of helicity of polypeptides containing protein amino acids from ellipticity values,[31] the helical content of these decapeptides can be calculated to be in the range of 25–35%. We believe that these values underestimate the actual amounts of helicity of our peptides because: 1) three (or four) out of ten amino acids in the sequences are achiral (Aib) residues, and 2) the main-chain length of the sequences (10 amino acids) is rather limited, thereby increasing the relative impact of terminal fraying (end effects).[28, 32, 33]

Membrane permeability properties: Trichogin GA IV, the prototypical lipopeptaibol, is known to exhibit a considerable membrane-perturbing activity.[3, 4, 34–37] It is even more destructive to small unilamellar vesicles of phosphatidyl choline and cholesterol than several longer nonlipidated peptaibols are. However, the details of the mechanism by which trichogin GA IV is able to release the aqueous content of small unilamellar liposomes are not clear yet.[3, 4, 36, 37] The membrane-modifying properties of the six 10-mer lipo-

 © 2003 Wiley-VCH Verlag GmbH & Co. KGaA, Weinheim

peptaibols **a** – **c** and **a′** – **c′**, tested by use of a liposome leakage assay, are compared in Figure 7 with those of the 10-mer trichogin GA IV (Oc-Aib-Gly-Leu-Aib-(Gly)$_2$-Leu-Aib-Gly-Ile-Lol) and its nonlipidated analogue (with Ac-Aib^0 and Leu(OMe)^{11}); the latter was taken as a negative control.[38] Notably, all of the compounds examined (except the negative control) are able to modify the artificial membrane. The enhanced capability of peptides **c** and **c′** for lysis should be associated with the increased hydrophobicity and helix stabilization imparted by the Etn^8 residue. The Glu(OMe) → Gln triple replacement seems beneficial, at least for peptides **a′** and **b′**. The naturally-occurring peptide LP237-F8 (peptide **c′**) is more active in the membranes than trichogin GA IV even though they have the same main-chain length. Thus, the observed difference might be related to the higher amphiphilic properties characterizing the 3D-structure of the former lipopeptaibol.

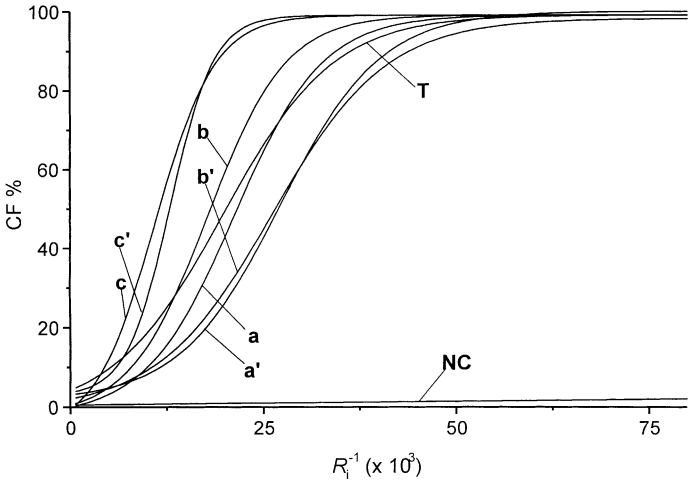

Figure 7. Peptide-induced carboxyfluorescein (CF) leakage after 20 min for different ratios R_i^{-1} = [peptide]/[lipid] ($\times 10^3$) from egg phosphatidyl choline/cholesterol (70:30) vesicles for the lipopeptaibol LP237-F8 (**c′**) and its five analogues (**a** – **c**, **a′**, and **b′**). A comparison is also made with the membrane activities of the prototypical lipopeptaibol trichogin GA IV (**T**) and the negative control analogue of trichogin GA IV (with Ac-Aib^0 and Leu-OMe^{11}; **NC**).[38]

Conclusion

In this work, by using the (*S*)-Etn residue obtained by asymmetric chemical synthesis, we prepared by solution methods the terminally blocked, 10-mer lipopeptaibol metabolite LP237-F8. Two analogues in which the Etn residue is replaced either by an Aib or a Nva residue have also been prepared. In solution, the three decapeptides are highly folded in helical structures. By combining high hydrophobicity and helix-stabilizing Cα-tetrasubstitution[9] at position 8, as in the naturally occurring, Etn-containing F8 metabolite, increased amphiphilicity and an associated, significantly higher capability for membrane lysis are obtained.

It is likely that additional lipopeptaibol mixtures with potent cytotoxic activity will be discovered in the near future. Furthermore, carefully tailored analogues of lipopeptaibols such as metabolite LP237-F8 are excellent tool components for biophysical studies of peptide – membrane interactions.[3, 4, 36]

Experimental Section

General for the synthesis and characterization of (*S*)-Etn: Melting points were determined on a Büchi SMP-20 capillary apparatus and are not corrected. IR absorption spectra were registered on a Perkin-Elmer 1600 FT-IR spectrophotometer. Optical rotations were measured in a cell with 10-cm pathlength on a Jasco P-1020 polarimeter. ^{1}H NMR (300 MHz) and ^{13}C NMR (75 MHz) spectra were recorded either with a Varian Unity-300 or Bruker ARX-300 spectrometer. Elemental analyses were obtained by using a Perkin-Elmer 2400 analyser.

(2*S*)-(1′*S*,2′*R*,4′*R*)-10′-(Dicyclohexylsulfamoyl)isobornyl-2-cyano-2-ethyl-4-pentenoate (2): Anhydrous potassium carbonate (3.45 g, 25 mmol) was added to a well-stirred solution of (2*RS*)-(1′*S*,2′*R*,4′*R*)-10′-(dicyclohexylsulfamoyl)isobornyl-2-cyanobutanoate (**1**)[39] (2.46 g, 5 mmol) and allyl bromide (1.21 g, 10 mmol) in dry acetone (60 mL). The resulting mixture was stirred at room temperature for 24 h and filtered, and the solid residue was washed with diethyl ether. The combined filtrates were concentrated in vacuo and the residue was dissolved in diethyl ether, washed with water, dried over anhydrous $MgSO_4$, filtered, and concentrated in vacuo to afford the corresponding (1′*S*,2′*R*,4′*R*)-10′-(dicyclohexylsulfamoyl)isobornyl-2-cyano-2-ethyl-4-pentenoate as a 90:10 mixture of diastereoisomers. Recrystallization from MeOH afforded the diastereomerically pure 2*S* compound in 62 % yield. M.p. 124 °C; ^{1}H NMR (300 MHz, $CDCl_3$, 25 °C): $\delta = 0.85$ (s, 3H; CH_3), 1.03 (s, 3H; CH_3), 1.12 (t, ^3J(H,H) = 7.5 Hz, 3H; CH_3), 1.10 – 2.20 (m, 29H; ethyl, isobornyl, $(Cy)_2$), 2.50 – 2.58 (m, 2H; CH_2–allyl), 2.57 (d, ^2J(H,H) = 13.2 Hz, 1H; $CHSO_2$), 3.22 – 3.36 (m, 2H; isobornyl), 3.38 (d, ^2J(H,H) = 13.2 Hz, 1H; $CHSO_2$), 4.94 (dd, ^3J(H,H) = 7.8, 3.0 Hz, 1H; CH–O), 5.15 – 5.26 (m, 2H; allyl); 5.74 – 5.90 (m, 1H; allyl) ppm; ^{13}C NMR (75 MHz, $CDCl_3$): $\delta = 9.6$, 19.9, 20.3, 22.9, 25.2, 26.2, 26.4, 27.0, 29.9, 30.7, 32.1, 33.5, 39.5, 41.4, 44.4, 49.3, 49.6, 49.7, 53.5, 57.3, 80.7, 119.0, 120.8, 130.8, 167.4 ppm; IR (Nujol): $\tilde{\nu} = 2244$ (C≡N), 1737 (C=O) cm^{-1}; elemental analysis calcd (%) for $C_{30}H_{48}N_2O_4S$: C 67.63, H 9.08, N 5.26, S 6.02; found: C 67.59, H 9.06, N 5.31, S 5.96.

(2*S*)-(1′*S*,2′*R*,4′*R*)-10′-(Dicyclohexylsulfamoyl)isobornyl-2-cyano-2-ethyl-pentanoate (3): ^{1}H NMR (300 MHz, $CDCl_3$, 25 °C): $\delta = 0.86$ (s, 3H; CH_3), 0.93 (t, ^3J(H,H) = 7.2 Hz, 3H; CH_3), 1.05 (s, 3H; CH_3), 1.12 (t, ^3J(H,H) = 7.5 Hz, 3H; CH_3), 1.16 – 2.20 (m, 31H; ethyl, isobornyl, $(Cy)_2$), 2.58 (d, ^2J(H,H) = 13.3 Hz, 1H; $CHSO_2$), 3.20 – 3.36 (m, 2H; isobornyl), 3.40 (d, ^2J(H,H) = 13.3 Hz, 1H; $CHSO_2$), 4.95 (dd, ^3J(H,H) = 7.8, 2.9 Hz, 1H; CH–O) ppm; ^{13}C NMR (75 MHz, $CDCl_3$): $\delta = 9.7$, 13.9, 18.8, 20.0, 20.4, 25.2, 26.2, 26.4, 27.0, 30.4, 30.7, 32.0, 33.5, 39.3, 39.6, 44.4, 49.4, 49.6, 50.1, 53.5, 57.4, 80.5, 119.6, 168.2; IR (Nujol): $\tilde{\nu} = 2240$ (C≡N), 1737 (C=O) cm^{-1}; elemental analysis calcd (%) for $C_{30}H_{50}N_2O_4S$: C 67.38, H 9.42, N 5.24, S 6.00; found: C 67.45, H 9.29, N 5.36, S 6.07.

(*S*)-2-Methoxycarbonylamino-2-ethylpentanonitrile (4): Oil; ^{1}H NMR (300 MHz, $CDCl_3$, 25 °C): $\delta = 0.95$ (t, ^3J(H,H) = 7.2 Hz, 3H; CH_3), 1.02 (t, ^3J(H,H) = 7.2 Hz, 3H; CH_3), 1.40 – 1.53 (m, 2H; CH_2), 1.79 – 1.88 (m, 2H; CH_2), 1.90 – 2.01 (m, 2H; CH_2), 3.70 (s, 3H; OCH_3), 4.81 (brs, 1H; NH) ppm; ^{13}C NMR ($CDCl_3$, 75 MHz): $\delta = 9.7$, 13.9, 16.3, 27.1, 33.7, 52.5, 57.4, 119.4, 155.2 ppm; IR (Nujol): $\tilde{\nu} = 3330$ (NH), 2238 (C≡N), 1715 (C=O) cm^{-1}; HR-MS (EI): calcd for $C_9H_{16}N_2O_2$: 184.1212; *m*/*z*: 184.1215 [*M*]$^+$.

(*S*)-2-Amino-2-ethylpentanoic acid (5): M.p. > 300 °C (decomp); $[\alpha]_D^{22} = +6.9$ ($c = 1$ in H_2O); ^{1}H NMR (300 MHz, D_2O, 25 °C): $\delta = 0.79$ (t, ^3J(H,H) = 7.2 Hz, 3H; CH_3), 0.79 (t, ^3J(H,H) = 7.5 Hz, 3H; CH_3), 1.08 – 1.10 (m, 1H; CH_2), 1.20 – 1.32 (m, 1H; CH_2), 1.50 – 1.82 (m, 4H; 2CH_2) ppm; ^{13}C NMR (75 MHz, D_2O): $\delta = 5.91$, 12.0, 15.3, 27.9, 36.8, 64.6, 174.9 ppm; IR (neat): $\tilde{\nu} = 3500 – 2000$ (NH), 1712 (C=O) cm^{-1}; elemental analysis calcd (%) for $C_7H_{15}NO_2$: C 57.90, H 10.41, N 9.65; found: C 57.83, H 10.48, N 9.57.

Synthesis and characterization of amino acid derivatives and peptides: The physical properties and analytical data for the newly synthesized amino acid derivatives and peptides are listed in Table 1. The syntheses and

© 2003 Wiley-VCH Verlag GmbH & Co. KGaA, Weinheim

characterization of Z-Aib-OH,[40–43] Oc-Aib-OH,[35] Boc-Aib-OBzl,[42] and Z-Ala-Leu-OMe[44] have already been reported.

FT-IR absorption spectroscopy: FT-IR absorption spectra were recorded with a Perkin-Elmer 1720X spectrophotometer, nitrogen flushed and equipped with a sample-shuttle device, at a nominal resolution of 2 cm^{-1}, averaging 100 scans. Solvent (baseline) spectra were recorded under the same conditions. Cells with path lengths of 0.1, 1.0, and 10 mm (with CaF_2 windows) were used. Spectrograde $CDCl_3$ (99.8% D) was purchased from Fluka.

NMR studies: NMR experiments were carried out on a Bruker Avance DMX-600 spectrometer. The peptide concentration was 3.5 mM in 0.3 M SDS-d_{25} and the sample temperature was 313 K. The water signal was suppressed by use of the WATERGATE pulse sequence. In all two dimensional experiments the spectra were acquired by collecting 500–512 runs, each one consisting of 64 scans and 4000 data points. The spin systems of protein amino acid residues were identified by using standard DQF-COSY and TOCSY experiments. In the latter case the spin-lock pulse sequence was 70 ms long. The stereospecific assignment of the Aib methyl group (except for Aib[8]) was obtained by means of semisoft NOESY experiments with digital resolution of 0.8 Hz per point in F1. A G4-shaped pulse, centered in the βH region, was used to replace the first 90° hard pulse. Normal NOESY experiments were used for specific sequence assignment. The mixing time of the NOESY experiments used for interproton distance determinations was 120 ms. Interproton distances were obtained by integration of the NOESY spectrum with the AURELIA software package.[45] Distances were calibrated on the peak between the two Phe βH protons, set to a distance of 1.78 Å. When peaks could not be integrated because of partial overlap, a distance corresponding to the maximum limit of detection of the experiment (4 Å) was assigned to the corresponding proton pair.

Structure calculations: Distance geometry (DG), molecular dynamics (MD), and simulated annealing (SA) protocol calculations were carried out by using the X-PLOR 3.1 program.[46] For distances involving equivalent or nonstereo assigned protons, r^{-6} averaging was used. The MD calculations involved a minimization stage of 100 cycles, followed by SA and refinement stages. The SA consisted of 30 ps of dynamics at 1500 K (10000 cycles in 3 fs steps) and of 30 ps of cooling from 1500 to 100 K in 50 K decrements (15000 cycles in 2 fs steps). The SA procedure, in which the weights of the NOE and nonbonded terms were gradually increased, was followed by 200 cycles of energy minimization. In the SA refinement stage the system was cooled from 1000 to 100 K in 50 K decrements (20000 cycles in 1 fs steps). Finally, the calculations were completed with 200 cycles of energy minimization with an NOE force constant of 50 kcal mol^{-1}. The generated structures were visualized by using the MOLMOL 2.6 program[47] with a Silicon Graphics O2 R 10000 workstation.

Circular dichroism: The CD spectra were obtained on a Jasco J-710 spectropolarimeter. Cylindrical, fused quartz cells of 10-, 1-, 0.2-, and 0.1-mm pathlength (Hellma) were used. The values are expressed in terms of $[\theta]_T$, the total molar ellipticity (deg × cm^2 × $dmol^{-1}$). Spectrograde MeOH (Baker) and 1,1,1,3,3,3-hexafluoroisopropanol (Acros Organics) were used as solvents. The peptide concentrations were determined by weight and the peptide content was obtained from quantitative amino acid analyses (C. Erba model 3A30) of the peptides.

Liposome leakage assay: Peptide-induced leakage from egg phosphatidyl choline (PC) vesicles was measured at 20 °C using the carboxyfluorescein (CF) entrapped vesicle technique as previously described.[48] CF-encapsulated small unilamellar vesicles (egg PC/cholesterol, 70:30) were prepared by sonication in 2-[4-(2-hydroxyethyl)-1-piperazinyl]ethanesulfonic acid (HEPES) buffer (pH 7.4). The phospholipid concentration was kept constant (0.6 mM), and increasing [peptide]/[lipid] molar ratios (R_i^{-1}) were obtained by adding aliquots of MeOH solutions of peptides, but keeping the final MeOH concentration below 5% by volume. After rapid and vigorous stirring, the time course of fluorescence change, corresponding to CF escape, was recorded at 520 nm (1 nm band pass) with $\lambda_{exc} = 488$ nm (1 nm band pass). The percentage of released CF at time t was determined as $(F_t - F_0)/(F_T - F_0) \times 100$, where F_0 = fluorescence intensity of vesicles in the absence of peptide, F_t = fluorescence intensity at time t in the presence of peptide, and F_T = total fluorescence intensity determined by disrupting the vesicles by addition of 30 µL of a 10% Triton X-100 solution. The kinetics studies were stopped at 20 min.

Acknowledgements

The authors gratefully acknowledge financial support for this research from the Spain–Italy exchange program "Accion Integrada" HI 97–20/"Azioni Integrate" 1997–1999.

[1] E. Benedetti, A. Bavoso, B. Di Blasio, V. Pavone, C. Pedone, C. Toniolo, G. M. Bonora, *Proc. Natl. Acad. Sci. USA* **1982**, *79*, 7951–7954.
[2] H. Brückner, H. Graf, *Experientia* **1983**, *39*, 528–530.
[3] S. Rebuffat, C. Goulard, B. Bodo, M.-F. Roquebert, *Recent Res. Devel. Org. Bioorg. Chem.* **1999**, *3*, 65–91.
[4] C. Toniolo, M. Crisma, F. Formaggio, C. Peggion, R. F. Epand, R. M. Epand, *Cell. Mol. Life Sci.* **2001**, *58*, 1179–1188.
[5] Y. S. Tsantrizos, S. Pischos, F. Sauriol, *J. Org. Chem.* **1996**, *61*, 2118–2121.
[6] Y. S. Tsantrizos, S. Pischos, F. Sauriol, P. Widden, *Can. J. Chem.* **1996**, *74*, 165–172.
[7] J. R. Cronin, S. Pizzarello, *Geochim. Cosmochim. Acta* **1986**, *50*, 2419–2425.
[8] C. J. Abshire, G. Planet, *J. Med. Chem.* **1972**, *15*, 226–229.
[9] C. Toniolo, M. Crisma, F. Formaggio, C. Peggion, *Biopolymers (Pept. Sci.)* **2001**, *60*, 396–419.
[10] C. Cativiela, M. D. Díaz-de-Villegas, *Tetrahedron: Asymmetry* **1998**, *9*, 3517–3599.
[11] R. Badorrey, C. Cativiela, M. D. Díaz-de-Villegas, J. A. Galvez, Y. Lapeña, *Tetrahedron: Asymmetry* **1997**, *8*, 311–317.
[12] F. Formaggio, Q. B. Broxterman, C. Toniolo in *Houben-Weyl, Methods of Organic Chemistry* (Eds.: M. Goodman, A. Felix, L. Moroder, C. Toniolo), Thieme, Stuttgart, **2003**, pp. 292–310.
[13] W. König, R. Geiger, *Chem. Ber.* **1970**, *103*, 788–798.
[14] L. A. Carpino, *J. Am. Chem. Soc.* **1993**, *115*, 4397–4398.
[15] H. C. Brown, S. Narasimhan, *J. Org. Chem.* **1982**, *47*, 1604–1606.
[16] M. Bodanszky, A. Bodanszky in *The Practice of Peptide Synthesis*, Springer, Berlin, **1984**, pp. 199–200.
[17] M. T. Cung, M. Marraud, J. Néel, *Ann. Chim. (Fr.)* **1972**, 183–209.
[18] M. Palumbo, S. Da Rin, G. M. Bonora, C. Toniolo, *Makromol. Chem.* **1976**, *177*, 1477–1492.
[19] G. M. Bonora, C. Mapelli, C. Toniolo, R. R. Wilkening, E. S. Stevens, *Int. J. Biol. Macromol.* **1984**, *6*, 179–188.
[20] G. Némethy, M. P. Printz, *Macromolecules* **1972**, *5*, 755–758.
[21] V. Pavone, G. Gaeta, A. Lombardi, F. Nastri, O. Maglio, C. Isernia, M. Saviano, *Biopolymers* **1996**, *38*, 705–721.
[22] K.-C. Chou, *Biopolymers* **1997**, *42*, 837–853.
[23] C. M. Venkatachalam, *Biopolymers* **1968**, *6*, 1425–1436.
[24] C. Toniolo, *C.R.C. Crit. Rev. Biochem.* **1980**, *9*, 1–44.
[25] G. D. Rose, L. M. Gierasch, J. A. Smith, *Adv. Protein Chem.* **1985**, *37*, 1–109.
[26] M. Bellanda, E. Peggion, R. Bürgi, W. Van Gunsteren, S. Mammi, *J. Peptide Res.* **2001**, *57*, 97–106.
[27] S. Beychok in *Poly-α-Amino Acids* (Ed.: G. D. Fasman), Dekker, New York, **1967**, pp. 293–337.
[28] M. Manning, R. W. Woody, *Biopolymers* **1991**, *31*, 569–586.
[29] C. Toniolo, A. Polese, F. Formaggio, M. Crisma, J. Kamphuis, *J. Am. Chem. Soc.* **1996**, *118*, 2744–2745.
[30] F. Formaggio, M. Crisma, P. Rossi, P. Scrimin, B. Kaptein, Q. B. Broxterman, J. Kamphuis, C. Toniolo, *Chem. Eur. J.* **2000**, *6*, 4498–4504.
[31] P. Walliman, R. J. Kennedy, D. S. Kemp, *Angew. Chem.* **1999**, *111*, 1377–1379; *Angew. Chem. Int. Ed.* **1999**, *38*, 1290–1292.
[32] T. S. Sudha, E. K. S. Vijayakumar, P. Balaram, *Int. J. Pept. Protein Res.* **1983**, *22*, 464–468.
[33] E. K. S. Vijayakumar, T. S. Sudha, P. Balaram, *Biopolymers* **1984**, *23*, 877–886.
[34] C. Auvin-Guette, S. Rebuffat, Y. Prigent, B. Bodo, *J. Am. Chem. Soc.* **1992**, *114*, 2170–2174.
[35] C. Toniolo, M. Crisma, F. Formaggio, C. Peggion, V. Monaco, S. Rebuffat, B. Bodo, *J. Am. Chem. Soc.* **1996**, *118*, 4952–4958.
[36] C. Peggion, F. Formaggio, M. Crisma, R. F. Epand, R. M. Epand, C. Toniolo, *J. Pept. Sci.* **2003**, in press.

 © 2003 Wiley-VCH Verlag GmbH & Co. KGaA, Weinheim

[37] L. Stella, C. Mazzuca, A. Palleschi, M. Venanzi, F. Formaggio, C. Toniolo, L. Moroder, B. Pispisa in *Peptides 2002* (Eds.: E. Benedetti, C. Pedone), Edizioni Ziino, Naples, **2002**, pp. 894 – 895.
[38] E. Locardi, S. Mammi, E. Peggion, V. Monaco, F. Formaggio, M. Crisma, C. Toniolo, B. Bodo, S. Rebuffat, J. Kamphuis, Q. B. Broxterman, *J. Pept. Sci.* **1998**, *4*, 389 – 399.
[39] C. Cativiela, M. D. Díaz-de-Villegas, J. A. Galvez, *J. Org. Chem.* **1994**, *59*, 2497 – 2505.
[40] M. T. Leplawy, D. S. Jones, G. W. Kenner, R. C. Sheppard, *Tetrahedron* **1960**, *11*, 39 – 51.
[41] W. J. McGahren, M. Goodman, *Tetrahedron* **1967**, *23*, 2017 – 2030.
[42] D. Leibfritz, E. Haupt, N. Dubischar, H. Lachmann, R. Oekonomopulos, G. Jung, *Tetrahedron* **1982**, *38*, 2165 – 2181.
[43] G. Valle, F. Formaggio, M. Crisma, G. M. Bonora, C. Toniolo, A. Bavoso, E. Benedetti, B. Di Blasio, V. Pavone, C. Pedone, *J. Chem. Soc. Perkin Trans. II* **1986**, 1371 – 1376.
[44] J. R. McDermott, N. L. Benoiton, *Can. J. Chem.* **1973**, *51*, 2555 – 2561.
[45] Dr. K. P. Neidig, *AURELIA software manual*, Karlsruhe, Germany, **1996**.
[46] A. T. Brunger, *X-PLOR Manual* (version 3.1), Yale University, CT, 1992.
[47] R. Koradi, M. Billeter, K. Wüthrich, *J. Mol. Graphics* **1996**, *14*, 51 – 55.
[48] M. El-Hajji, S. Rebuffat, T. Le Doan, G. Klein, M. Satre, B. Bodo, *Biochim. Biophys. Acta* **1989**, *978*, 97 – 104.

Received: January 22, 2003
Revised: April 16, 2003 [F4756]

© 2003 Wiley-VCH Verlag GmbH & Co. KGaA, Weinheim